


ORIGINAL ARTICLE

Binding characterization of *N*-(2-chloro-5-thiomethylphenyl)-*N'*-(3-[³H]methoxy phenyl)-*N'*-methylguanidine ([³H]GMOM), a non-competitive *N*-methyl-D-aspartate (NMDA) receptor antagonist

Athanasios Metaxas  | Bart N. M. van Berckel | Pieter J. Klein | Joost Verbeek | Emily C. Nash | Esther J. M. Kooijman | Véronique A. Renjaän | Sandeep S. V. Golla | Ronald Boellaard | Johannes A. M. Christiaans | Albert D. Windhorst | José E. Leysen

Department of Radiology & Nuclear Medicine, Neuroscience Campus Amsterdam, VU University Medical Center, Amsterdam, the Netherlands

Correspondence

Athanasios Metaxas, Department of Neurobiology Research, Institution of Molecular Medicine, University of Southern Denmark, Odense, Denmark.
Email: ametaxas@health.sdu.dk

Funding information

Center for Translational Molecular Medicine; EU 7th Framework program EURIPIDES

Abstract

Labeled with carbon-11, *N*-(2-chloro-5-thiomethylphenyl)-*N'*-(3-methoxyphenyl)-*N'*-methylguanidine ([¹¹C]GMOM) is currently the only positron emission tomography (PET) tracer that has shown selectivity for the ion-channel site of *N*-methyl-D-aspartate (NMDA) receptors in human imaging studies. The present study reports on the selectivity profile and in vitro binding properties of GMOM. The compound was screened on a panel of 80 targets, and labeled with tritium ([³H]GMOM). The binding properties of [³H]GMOM were compared to those of the reference ion-channel ligand [³H](+)-dizocilpine maleate ([³H]MK-801), in a set of concentration-response, homologous and heterologous inhibition, and association kinetics assays, performed with repeatedly washed rat forebrain preparations. GMOM was at least 70-fold more selective for NMDA receptors compared to all other targets examined. In homologous inhibition and concentration-response assays, the binding of [³H]GMOM was regulated by NMDA receptor agonists, albeit in a less prominent manner compared to [³H]MK-801. Scatchard transformation of homologous inhibition data produced concave upward curves for [³H]GMOM and [³H]MK-801. The radioligands showed bi-exponential association kinetics in the presence of 100 μmol L⁻¹ L-glutamate/30 μmol L⁻¹ glycine. [³H]GMOM (3 nmol L⁻¹ and 10 nmol L⁻¹) was inhibited with dual affinity by (+)-MK-801, (*R,S*)-ketamine and memantine, in both presence and absence of agonists. [³H]MK-801 (2 nmol L⁻¹) was inhibited in a monophasic manner by GMOM under baseline and combined agonist conditions,

Abbreviations: CGP 78608, [(1*S*)-1-[[[7-Bromo-1,2,3,4-tetrahydro-2,3-dioxo-5-quinolalyl] methyl]amino]ethyl]phosphonic acid; CNS-5161, *N*-(2-chloro-5-thiomethylphenyl)-*N'*-(3-thiomethylphenyl)-*N'*-methylguanidine; D-AP5, D-(-)-2-Amino-5-phosphono pentanoic acid; DMF, *N,N*-dimethylformamide; DMSO, dimethyl sulfoxide; GE-179, *N*-(2-chloro-5-(2-fluoroethylthiophenyl)-*N'*-(3-thiomethylphenyl)-*N'*-methylguanidine; GMOM, *N*-(2-chloro-5-thiomethylphenyl)-*N'*-(3-methoxyphenyl)-*N'*-methylguanidine; HPLC, high-performance liquid chromatography; IC₅₀, half-maximal inhibitory concentration; K_d, equilibrium dissociation constant; K_i, inhibition constant; K_i, net influx rate; k_{ob}, observed kinetic rate constant; LSD, least significant difference; MK-801, dizocilpine; nH, Hill coefficient; NMDA, *N*-methyl-D-aspartate; NSB, non-specific binding; PEI, polyethyleneimine; PET, positron emission tomography; PK-209, *N*-(2-chloro-5-thiomethylphenyl)-*N'*-(3-fluoromethoxyphenyl)-*N'*-methylguanidine; TCP, thienyl cyclohexylpiperidine; V_{ND}, volume of distribution (non-displaceable).

This is an open access article under the terms of the Creative Commons Attribution-NonCommercial-NoDerivs License, which permits use and distribution in any medium, provided the original work is properly cited, the use is non-commercial and no modifications or adaptations are made.

© 2019 The Authors. *Pharmacology Research & Perspectives* published by John Wiley & Sons Ltd, British Pharmacological Society and American Society for Pharmacology and Experimental Therapeutics.

with an IC_{50} value of ~ 19 nmol L^{-1} . The non-linear Scatchard plots, biphasic inhibition by open channel blockers, and bi-exponential kinetics of [3H]GMOM indicate a complex mechanism of interaction with the NMDA receptor ionophore. The implications for quantifying the PET signal of [^{11}C]GMOM are discussed.

KEYWORDS

[3H]GMOM, [3H]MK-801, binding, ion-channel, *N*, *N'*-diaryl-*N*-methylguanidine, NMDA receptor

1 | INTRODUCTION

N-methyl-D-aspartate (NMDA) receptors are actively being pursued as imaging targets for the development of positron emission tomography (PET) tracers.^{1,2} A PET imaging probe for the NMDA receptors can be used for the diagnosis and monitoring of a range of neurological and psychiatric disorders involving NMDA receptor dysfunction, including neuropathic pain, epilepsy, stroke, neurodegenerative diseases, and schizophrenia.³

The ionotropic NMDA receptors possess at least six distinct sites for the recognition of endogenous ligands, including sites for the agonist L-glutamate, the co-agonists glycine and D-serine, and modulators of receptor function as diverse as polyamines, steroids, metal ions, and protons.⁴ Of the multiple binding sites, considerable effort has been directed on imaging the site within the pore of the NMDA receptor ion-channel. Due to its unique physical location, the intra-channel site is primarily accessible when the NMDA receptors are in an open conformation, that is activated by the agonists L-glutamate and glycine/D-serine.^{5,6} Thus, PET tracer uptake at the ion-channel

site should be proportional to the amount of activated NMDA receptors, permitting the evaluation of their functional state *in vivo*.⁷

N, *N'*-di-substituted guanidines were first described as open channel blockers of the NMDA receptors by electrophysiology, in 1989.⁸ To date, diarylguanidine analogs constitute the most promising class of compounds for the functional imaging of NMDA receptors. Unlike early derivatives of phencyclidine and (+)-dizocilpine maleate (MK-801), which were unsuitable for PET due to high lipophilicity and non-specific uptake,⁹⁻¹¹ *N*-(2-chloro-5-thiomethylphenyl)-*N'*-(3-[^{11}C]methoxyphenyl)-*N'*-methylguanidine ([^{11}C]GMOM)¹² *N*-(2-chloro-5-thiomethylphenyl)-*N'*-(3-[^{18}F]fluoromethoxyphenyl)-*N'*-methylguanidine ([^{18}F]PK-209)¹³ *N*-(2-chloro-5-thiomethylphenyl)-*N'*-(3-thiomethylphenyl)-*N'*-[^{11}C]methylguanidine ([^{11}C]CNS-5161)¹⁴ and *N*-(2-chloro-5-(2-[^{18}F]fluoroethylthiophenyl)-*N'*-(3-thiomethylphenyl)-*N*-methylguanidine ([^{18}F]GE-179)¹⁵ are NMDA-targeting tracers of moderate lipophilicity and high affinity (Figure 1), which have exhibited quantifiable brain uptake in human PET studies).¹⁶⁻¹⁹ [^{11}C]GMOM, in particular, is currently the only diarylguanidine tracer that has shown selectivity for the NMDA receptors *in vivo*, as evidenced by a

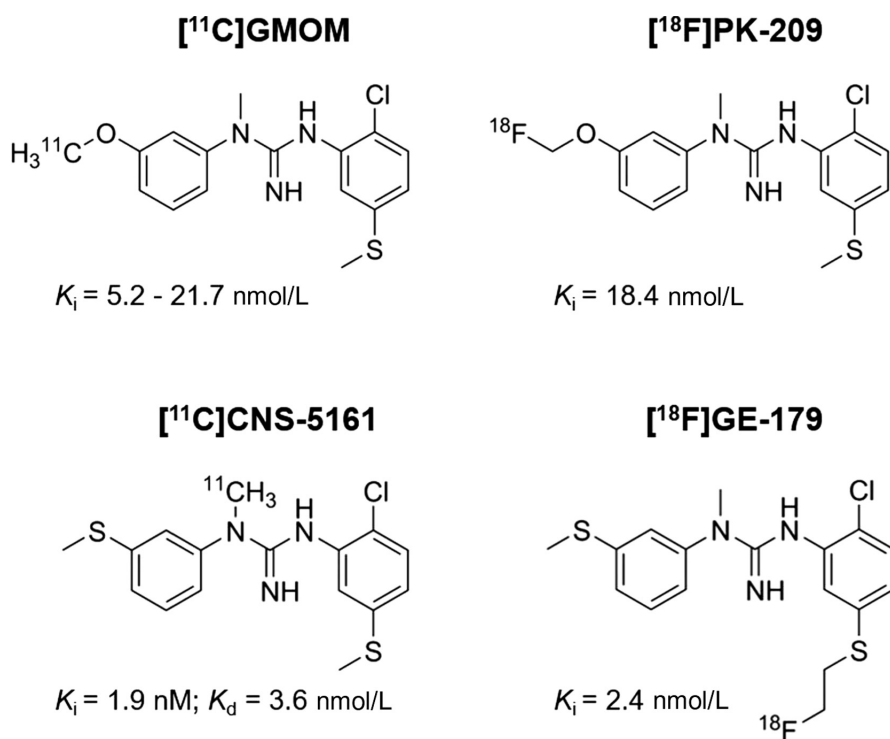


FIGURE 1 Structures and affinity values of NMDA receptor PET tracers used in human imaging studies

reduction in the tracer's net influx rate following the administration of an S-ketamine challenge to healthy human volunteers.¹⁹

Despite showing considerable potential as a PET tracer, [¹¹C]GMOM remains poorly characterized in terms of its in vitro binding profile. GMOM is known to possess a high-affinity binding site that is associated with the reference ion-channel blocker of NMDA receptors, [³H](+)-dizocilpine maleate ([³H]MK-801). In competition binding assays against [³H]MK-801, the inhibition constant (K_i) of GMOM has been reported to range from 5.2 nmol L⁻¹ to 21.7 nmol L⁻¹.^{12,13} Apart from this information, however, no further details on GMOM's interaction with the NMDA receptor channel are currently available.

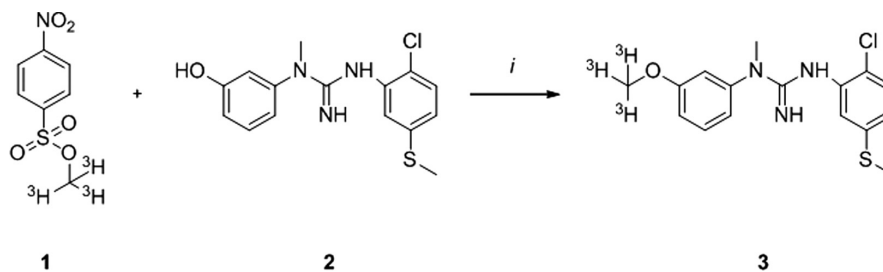
The goal of the present study was to examine the selectivity and in vitro binding properties of the diarylguanidine GMOM. The compound was labeled with tritium ([³H]GMOM), and its binding profile compared with that of [³H]MK-801 in a set of concentration-response, inhibition, and association kinetics experiments.

2 | MATERIALS AND METHODS

2.1 | Selectivity profile of GMOM

The pharmacological selectivity of GMOM was evaluated at CEREP S.A. (Poitiers, France), using a broad screen of 79 targets, comprising neurotransmitter receptors and transporters, and ion-channels (Table S1). Binding of GMOM to the ifenprodil site of NMDA receptors was evaluated in-house, using a previously detailed assay.²⁰ A percent (%) inhibition of control specific binding was initially calculated for each target, using a single concentration of GMOM (10 μmol L⁻¹). The affinity of GMOM for targets showing ≥50% inhibition of control binding in the primary screen was subsequently derived from full concentration-response inhibition curves, which were obtained by using at least eight concentrations of GMOM. Hill coefficients (nH) and half-maximal inhibitory concentrations (IC₅₀) were derived from the competition binding experiments by non-linear regression analysis, using software developed at CEREP (Hill software). IC₅₀ values were converted to inhibitory constant values (K_i) with the Cheng and Prusoff²¹ equation for binding assays: $K_i = IC_{50}/(1 + [L]/K_d)$, where [L] is radioligand concentration in the assay and K_d the equilibrium dissociation constant of the radioligand for its corresponding target. The K_d values of the reference radioligands were obtained from saturation binding experiments, which were run in parallel to the competition studies. Details of the CEREP selectivity assays are available from www.cerep.fr.

SCHEME 1 Synthesis of [³H]GMOM. (1) [³H]methyl nosylate. (2) N-(2-chloro-5-thiomethylphenyl)-N'-(3-hydroxyphenyl)-N'-[(3-³H)₃ methoxyphenyl]-N'-methylguanidine. (3) N-(2-chloro-5-thiomethylphenyl)-N'-(3-³H)₃ methoxyphenyl)-N'-methylguanidine ([³H]GMOM). *i*: DMF, NaOH (5 mol L⁻¹), 80°C, 30 minutes



2.2 | Synthesis of [³H]GMOM

[³H]GMOM was synthesized by reaction of the OH-precursor [3-(2-chloro-5-(methylthio)phenyl)-1-(3-hydroxyphenyl)-1-methylguanidine;¹³] with [³H]methyl nosylate (specific activity [SA]: 84.5 Ci/mmol; PerkinElmer, Waltham, MA) and NaOH as base (Scheme 1). [³H]methyl nosylate in hexane/ethyl acetate (50 MBq) was injected into a closed, screw-cap reaction vial. After evaporating the solvent under a gentle flow of argon at 80°C, 1 mg (3.1 μmol) of precursor in 400 μL dry N,N-dimethylformamide (DMF) and 2 μL NaOH (5 mol L⁻¹) were added to the reaction vessel. Following incubation at 80°C for 30 min, the reaction was cooled to room temperature and quenched with 500 μL sterile H₂O. For semi-preparative high-performance liquid chromatography (HPLC) purification, the complete reaction mixture was passed over an Altima C18 column (10 × 250 mm, 5 μm; Grace Alltech, Breda, the Netherlands), and eluted at a flow rate of 4 mL·min⁻¹ with acetonitrile/50 mmol L⁻¹ NH₄H₂PO₄ in H₂O (pH 2.5), 50/50 (v/v). UV monitoring was set at 254 nm (UV-1575, Jasco Benelux, de Meern, the Netherlands). Fractions were collected at 1 min intervals, and a 5 μL aliquot from each fraction was added into 5 mL scintillation liquid (Optiphase-HiSafe 3; PerkinElmer, Groningen, the Netherlands) and measured for 1 min in a RackBeta 1219 counter (LKB-Wallac, Turku, Finland). The fractions containing [³H]GMOM were diluted with 45 mL H₂O (1:10) and passed over a preconditioned tC18 plus Sep-Pak (Waters Chromatography, Etten-Leur, the Netherlands), to remove acetonitrile and concentrate the product solution. The cartridge was rinsed twice with 10 mL H₂O, and [³H]GMOM was obtained by elution with 1.5 mL ethanol (96%; Biosolve, Valkenswaard, the Netherlands). For analytical HPLC, [³H]GMOM was passed over a Platinum C18EPS column (4.6 × 250 mm, 5 μm, Grace Alltech), and eluted at a flow rate of 1 mL·min⁻¹ with methanol/50 mmol L⁻¹ NH₄H₂PO₄ in H₂O (pH 2.5), 70/30 (v/v). HPLC effluents were monitored using an online UV detector (254 nm) and a radioactivity detector (LABLogic β-RAM model 4, MetorX, Goedereede, the Netherlands), connected in series.

2.3 | Animals and membrane preparation

All procedures complied with European Commission Directive 2010/63/EU, regulating animal research, and were approved by the institutional animal ethics committee of the VUmc. Male Wistar rats (140–160 g) were purchased from Harlan Laboratories, Venray, the Netherlands. The animals were housed in groups of 4, under a 12 hour light-

dark cycle (lights on: 8 AM) and controlled temperature ($21 \pm 2^\circ\text{C}$) and humidity conditions ($50 \pm 10\%$). Food and water were available ad libitum (Teklad Global 16% Protein Rodent Diet, Harlan Laboratories).

Extensively washed, crude synaptic membranes were prepared as detailed previously.²² Animals were killed by decapitation, and the cerebral cortices and hippocampi immediately removed and homogenized in a 15-fold excess (v/w) of ice-cold 0.32 mol L^{-1} sucrose, using a DUALL tissue grinder (20 strokes, 800 rpm; VWR, Amsterdam, the Netherlands). The homogenate was centrifuged at 1000 g for 10 minutes in a refrigerated centrifuge (rotor 70 Ti; Beckman-Coulter Nederland B.V., Woerden, the Netherlands). The supernatant was decanted and centrifuged for 20 minutes at $20\,000 \text{ g}$. The resulting pellet was suspended in 30 vol of ice-cold, ultra-pure Milli-Q water (dH_2O ; Merck Millipore, Amsterdam, the Netherlands) by using an Ultra-Turrax homogenizer (T18 digital, IKA, Staufen im Breisgau, Germany), and centrifuged for 20 minutes at 8000 g . The supernatant and buffy layer were removed and re-centrifuged at $165\,000 \text{ g}$ for 20 minutes. The membrane pellets were suspended in 30 vol of 5 mmol L^{-1} EDTA- 15 mmol L^{-1} Tris solution (pH 7.4) and incubated at 37°C for 1 hour. Following incubation, the suspension was centrifuged at $165\,000 \text{ g}$ for 20 minutes, and the pellets frozen at -80°C for 1-3 days. For binding experiments, the pellets were thawed to room temperature and suspended in 30 vol of dH_2O . The membrane suspension was incubated at 37°C for 1 hour and washed twice for 30 minutes at $165\,000 \text{ g}$. After the final centrifugation step, pellets were diluted in 80 vol of assay buffer (5 mmol L^{-1} Tris-HCl, pH 7.4), corresponding to $\sim 5 \text{ mg}$ of wet tissue weight, and used in radioligand binding assays. Protein concentration was determined with the BCA protein kit, and bovine serum albumin as standard (ThermoFisher Scientific, Breda, the Netherlands).

2.4 | Binding studies

2.4.1 | Optimization of binding conditions

Whatman GF/B filters (AlphaBiotec, Glasgow, UK) were presoaked for 1 hour in assay buffer with or without 0.15% polyethyleneimine (PEI), to evaluate binding of 2 nmol L^{-1} [^3H]GMOM and [^3H]MK-801 (SA: 22.5 Ci/mmol; PerkinElmer, Waltham, MA) to the glass fiber filters (no added membrane). The stability of specific radioligand binding at 25°C was evaluated after incubating [^3H]GMOM and [^3H]MK-801 with the extensively washed membrane suspension for 30 minutes, 4 hours and 24 hours, in the presence of $100 \mu\text{mol L}^{-1}$ L-glutamic acid (L-glutamate) and $30 \mu\text{mol L}^{-1}$ glycine (Sigma-Aldrich, Zwijndrecht, the Netherlands). A tissue dilution curve was performed to determine linearity of specific binding vs membrane protein concentration, following 2 hours incubations in the presence of $100 \mu\text{mol L}^{-1}$ L-glutamate and $30 \mu\text{mol L}^{-1}$ glycine (25°C). Specific radioligand binding to heat-denatured membranes was assessed after exposing the membrane suspension to 80°C for 10 minutes. (*R,S*)-ketamine HCl ($500 \mu\text{mol L}^{-1}$; Duchefa Farma BV, Haarlem, the Netherlands) was used to define non-specific binding (NSB) in these preliminary studies. The pH dependence of [^3H]GMOM binding (2 nmol L^{-1}) was assessed under baseline conditions (no added L-glutamate/glycine) following 20 hours

incubations in assay buffer, using $10 \mu\text{mol L}^{-1}$ unlabeled GMOM to define NSB (pH range: 6.5-8.5). Based on these preliminary studies, the methods described below represent optimized binding conditions.

2.4.2 | Regulation of radioligand binding by NMDA receptor agonists/antagonists

The effects of L-glutamate and glycine on the binding of 10 nmol L^{-1} [^3H]GMOM and 2.5 nmol L^{-1} [^3H]MK-801 were examined by directly incubating the extensively washed membrane suspension (no freeze-thaw cycle) with increasing concentrations of the amino acids (final concentration range: 1 nmol L^{-1} - $100 \mu\text{mol L}^{-1}$). In addition, radioligand binding was measured in the presence of the GluN2 subunit agonists NMDA and (*R,S*)-(Tetrazol-5-yl)glycine, and the orthosteric antagonists [(1*S*)-1-[[[7-Bromo-1,2,3,4-tetrahydro-2,3-dioxo-5-quinoxaliny]methyl]amino]ethyl]phosphonic acid hydrochloride (CGP 78608 HCl) and D-(-)-2-Amino-5-phosphono pentanoic acid (D-AP5; Tocris Bioscience, Bristol, UK), which were tested at concentrations spanning ~ 1 , 2 and $10\times$ their respective affinity values for the different subunits of the NMDA receptor.²³⁻²⁵ Incubations were carried out overnight (~ 20 hours) in a shaking water bath (25°C), in a final assay volume of $500 \mu\text{L}$, composed of $400 \mu\text{L}$ freshly prepared membrane suspension, $50 \mu\text{L}$ assay buffer with and without agonists/antagonists, and $50 \mu\text{L}$ of radioligand in assay buffer (5 mmol L^{-1} Tris-HCl; pH 7.4). The binding reactions were stopped by vacuum filtration through Whatman GF/B filters, pre-soaked for 1 hour in 0.15% PEI. The filters were washed three times with 3 mL of ice-cold assay buffer (pH 7.4), all procedures carried out using a 48-well Brandel harvester (AlphaBiotec). Filter disks were placed in 5 mL scintillation liquid (Optiphase Hisafe 3; PerkinElmer, the Netherlands), and shaken vigorously overnight. Bound radioactivity was counted for 1 minute in a RackBeta 1219 scintillation counter (LKB-Wallac), at a measured efficiency of 40%.

For evaluating half-maximal effective agonist concentrations (EC_{50}) from the L-glutamate and glycine response curves, data were fitted to the log(agonist) vs normalized response equation (variable slope), built into GraphPad Prism (v6.0; GraphPad Software Inc., San Diego, CA). Experiments were conducted in triplicate, 3-4 independent times.

2.4.3 | Homologous inhibition studies

For self-inhibition assays, the extensively washed membrane suspension was incubated with [^3H]GMOM ($1-3 \text{ nmol L}^{-1}$; SA: 84.5 Ci/mmol) and increasing concentrations of unlabeled GMOM fumaric acid (base MW: 335.85). Incubations were conducted in the absence and presence of $100 \mu\text{mol L}^{-1}$ L-glutamate, $30 \mu\text{mol L}^{-1}$ glycine (Sigma-Aldrich), and $100 \mu\text{mol L}^{-1}$ L-glutamate plus $30 \mu\text{mol L}^{-1}$ glycine. For comparison purposes, a parallel series of experiments was performed under each incubation condition, by using [^3H]MK-801 ($2-3 \text{ nmol L}^{-1}$; SA: 22.5 Ci/mmol) and unlabeled MK-801 for inhibition (base MW: 337.37; Sigma-Aldrich). "Cold" ligands were dissolved as 10 mmol L^{-1} stock solutions in DMSO, and used in a concentration range of 10 pmol L^{-1} - $10 \mu\text{mol L}^{-1}$. Incubations were carried out in a final assay

volume of 500 μL , comprising 400 μL membrane suspension (protein concentration range: 120–180 $\mu\text{g}\cdot\text{mL}^{-1}$), 45 μL assay buffer (5 mmol L^{-1} Tris-HCl, pH 7.4), 5 μL unlabeled GMOM or MK-801 (final DMSO concentration: 1%), and 50 μL radioligand in assay buffer (final ethanol concentration: <0.1%).

K_d values and maximal number of binding sites (B_{max}) for [^3H]GMOM and [^3H]MK-801 were calculated by non-linear regression analysis, using a one-site homologous competition model built into GraphPad Prism. Scatchard transformations were performed as detailed previously,²⁶ by using 100 $\mu\text{mol L}^{-1}$ of unlabeled GMOM and MK-801 to define NSB. Linear regression of the Scatchard plots was used to compute radioligand K_d and B_{max} values. Experiments were performed 4–6 times independently, each conducted in triplicate.

2.4.4 | Heterologous inhibition studies

The ability of increasing concentrations of MK-801 (10 pmol L^{-1} –100 $\mu\text{mol L}^{-1}$; Sigma-Aldrich), (*R,S*)-ketamine HCl (1 nmol L^{-1} –10 mmol L^{-1}), memantine HCl (1 nmol L^{-1} –1 mmol L^{-1} ; Tocris Bioscience) and CNS-5161 (1 pmol L^{-1} –100 $\mu\text{mol L}^{-1}$; ABX GmbH, Germany) to inhibit the binding of 3 nmol L^{-1} [^3H]GMOM was examined in both absence and presence of 100 $\mu\text{mol L}^{-1}$ L -glutamate and 30 $\mu\text{mol L}^{-1}$ glycine. MK-801, (*R,S*)-ketamine, memantine and CNS-5161 were further tested against 10 nmol L^{-1} [^3H]GMOM, in the presence of L -glutamate/glycine. GMOM, memantine, (*R,S*)-ketamine and CNS-5161 were tested against 2 nmol L^{-1} [^3H]MK-801, under both baseline and L -glutamate/glycine conditions.

All competitors were dissolved as 10 mmol L^{-1} stock solutions in DMSO, with the exception of (*R,S*)-ketamine, which was prepared as 1 mol L^{-1} stock solution in dH_2O , containing 10% ethanol. Experiments were repeated 3–9 independent times. IC_{50} values were derived from the concentration-inhibition curves by fitting the raw data to the one- or two-sites competition model using GraphPad Prism software. All values were calculated as $\log\text{IC}_{50}$ and reported as the IC_{50} .

2.4.5 | Association kinetics

Observed kinetic rate constants (k_{ob}) were determined with 5 nmol L^{-1} , 10 nmol L^{-1} , and 20 nmol L^{-1} of [^3H]GMOM (SA: 20 Ci/mmol) and 1 nmol L^{-1} , 2.5 nmol L^{-1} and 5 nmol L^{-1} of [^3H]MK-801, in the presence of combined L -glutamate (100 $\mu\text{mol L}^{-1}$) and glycine (30 $\mu\text{mol L}^{-1}$). Non-specific binding was defined as that remaining in the presence of 500 $\mu\text{mol L}^{-1}$ (*R,S*)-ketamine HCl. Time-points ranging from 30 seconds up to 480 minutes were evaluated. Experiments were conducted in triplicate, three independent times. Data were analyzed using the one- or two-phase exponential association model built into GraphPad Prism.

2.5 | Data and statistical analysis

The equations used for analysis are shown in Supplementary Materials and Methods. Two-tailed independent *t* tests were used to compare EC_{50} values and the maximal effects of L -glutamate/glycine on

the binding of [^3H]GMOM and [^3H]MK-801. Two-way ANOVA for the independent factors radioligand type and incubation condition (or regulator concentration) was used to compare B_{max} and K_d values, as well as the effect of NMDA receptor agonism/antagonism on the binding of [^3H]GMOM and [^3H]MK-801. Observed association rate constants (k_{ob}) for each radioligand, derived by analyzing total and specific binding values, were compared by repeated measures ANOVA. Where ANOVA yielded significant effects, data were further analyzed by Fisher's Least Significant Difference (LSD) post-hoc tests. IC_{50} values from the heterologous inhibition assays were compared between baseline and L -glutamate/glycine conditions by using independent *t* tests (two-tailed). When one- or two-site models were considered, data fits were compared by visual inspection of the corresponding curves, and model preference assessed by the Akaike method. Results are reported as the mean \pm standard error of the mean (SEM) of *n* independent experiments, each conducted in triplicate.

3 | RESULTS

3.1 | Selectivity profile of GMOM

GMOM at 10 $\mu\text{mol L}^{-1}$ inhibited less than 50% of control specific binding at 69 of the 80 targets tested, including the glutamate (4% inhibition), glycine (no inhibition), and ifenprodil binding sites of the NMDA receptor (23% inhibition). Affinity values for targets showing $\geq 50\%$ inhibition of control binding in the primary screen are listed in Table 1. In freshly prepared membranes from the rat cerebral cortex, GMOM inhibited the binding of [^3H]thienyl-cyclohexylpiperidine ([^3H]TCP; 10 nmol L^{-1}) with a K_i value of 15 nmol L^{-1} . The selectivity of GMOM for the NMDA receptor ion-channel was at least 70-fold higher compared to all other targets examined.

3.2 | Synthesis of [^3H]GMOM

Five to ten MBq of [^3H]GMOM were obtained per synthesis, with radiochemical yields ranging from 11 to 22%. The specific activity of the product was 3.13 TBq/mmol (84.5 Ci/mmol), and its radiochemical and chemical purity >99% (Figure 2).

3.3 | Binding conditions

A fraction of [^3H]GMOM binding ($\sim 2.5\%$) represented non-specific binding to the glass fiber filters, and was reduced by incubating the GF/B filters for 1 hour in assay buffer, containing 0.15% PEI (Figure 3A). With PEI pretreated filters, specific radioligand binding accounted for 76.4% of the total binding of 2 nmol L^{-1} [^3H]GMOM and 83.5% of the total binding of 2 nmol L^{-1} [^3H]MK-801. Radioligand binding was stable for at least 24 hours at 25°C (Figure 3B), showing a linear relationship with wet tissue weights between 2.5 mg and 20 mg per assay (Figure 3C). The binding of [^3H]GMOM was heat-labile (Figure 3D) and pH-dependent (Figure 3E), with optimum binding occurring at pH 7.4.

TABLE 1 Affinity values (IC_{50}/K_i) and Hill coefficients (nH) of GMOM for targets showing $\geq 50\%$ inhibition of control specific binding in the primary screen

Target	IC_{50} (M) ^a	K_i (M) ^b	nH ^c
1 Adrenergic alpha 1A	4.4×10^{-6}	2.2×10^{-6}	-0.9
2 Melatonin 1A	3.0×10^{-6}	2.4×10^{-6}	-0.7
3 Muscarinic M1	4.9×10^{-6}	4.2×10^{-6}	-1.0
4 Muscarinic M2	3.5×10^{-6}	2.4×10^{-6}	-1.0
5 Opioid κ (KOP)	5.0×10^{-6}	3.3×10^{-6}	-0.8
6 Opioid μ (MOP)	2.7×10^{-6}	1.1×10^{-6}	-1.0
7 NMDA (PCP site)	2.7×10^{-8}	1.5×10^{-8}	-1.1
8 Serotonin 2B (5-HT2B)	5.6×10^{-6}	2.8×10^{-6}	-1.0
9 Sigma (1 and 2)	2.2×10^{-6}	1.7×10^{-6}	-0.9
10 Ca^{2+} channel (L, verapamil site)	2.2×10^{-6}	1.1×10^{-6}	-0.8
11 Na^+ channel (site 2)	3.9×10^{-6}	3.6×10^{-6}	-0.9

^a IC_{50} is the concentration of GMOM inhibiting 50% of radioligand binding to the target of interest.

^b K_i was obtained by transforming IC_{50} values according to the Cheng and Prusoff equation. For the transformation, K_d values of the reference radioligands were obtained from saturation binding experiments, which were run in parallel to the competition studies.

^cnH is the slope factor of the inhibition curve (Hill coefficient).

3.4 | Regulation of radioligand binding by NMDA receptor agonists/antagonists

The binding of [³H]GMOM (10 nmol L⁻¹) and [³H]MK-801 (2.5 nmol L⁻¹) to extensively washed membranes was examined at increasing concentrations of L-glutamate and glycine (range: 1 nmol L⁻¹-

100 μ mol L⁻¹; Figure 4 A and B). For [³H]MK-801, the maximal glutamate-induced increase over baseline binding levels was $171.4 \pm 7.5\%$, observed at an agonist concentration range between 10-100 μ mol L⁻¹. For [³H]GMOM, the maximal effect of L-glutamate was lower than that of [³H]MK801 ($55.8 \pm 6.0\%$; $t_4 = 12.0$; $P < 0.001$) and occurred over the same agonist concentration range (10-100 μ mol L⁻¹). The EC_{50} values for glutamate-induced binding enhancement were $0.20 \pm 0.01 \mu$ mol L⁻¹ for [³H]MK-801 and $0.23 \pm 0.08 \mu$ mol L⁻¹ for [³H]GMOM ($t_4 = 1.3$; $P > 0.05$). Glycine increased the binding of [³H]MK-801 by $121.8 \pm 19.2\%$ from control levels, with an EC_{50} value of $1.05 \pm 0.50 \mu$ mol L⁻¹ (Figure 4B). For [³H]GMOM, the effects of glycine did not plateau at concentrations as high as 100 μ mol L⁻¹. The agonist induced small, concentration-dependent effects on the binding levels of [³H]GMOM, which were increased by $\sim 45\%$ at 1 nmol L⁻¹ vs 100 μ mol L⁻¹ glycine ($t_{16} = 6.9$; $P < 0.001$).

The differential sensitivity of [³H]GMOM and [³H]MK-801 to NMDA receptor agonism was confirmed by using NMDA ($F_{1,12} = 51.2$, $P < 0.001$) and (R,S)-(Tetrazol-5-yl)glycine ($F_{1,12} = 39.9$, $P < 0.001$; Figure 4C). Both agonists produced concentration-dependent increases in the binding of [³H]MK-801 and [³H]GMOM ($F_{2,12} = 4.5$, $P < 0.05$). However, at each concentration examined, agonist-induced effects were more pronounced for [³H]MK-801 than [³H]GMOM (Figure 4C; LSD post-hoc tests). The orthosteric antagonists GCP 78608 ($F_{2,18} = 8.2$, $P < 0.01$) and D-AP5 ($F_{2,16} = 15.3$, $P < 0.001$) caused concentration-dependent inhibition of binding, which was more pronounced for [³H]MK-801 than [³H]GMOM ($F_{1,16} = 17.7$, $P < 0.001$ for D-AP; $F_{1,18} = 6.1$, $P < 0.05$ for GCP 78608; Figure 4D).

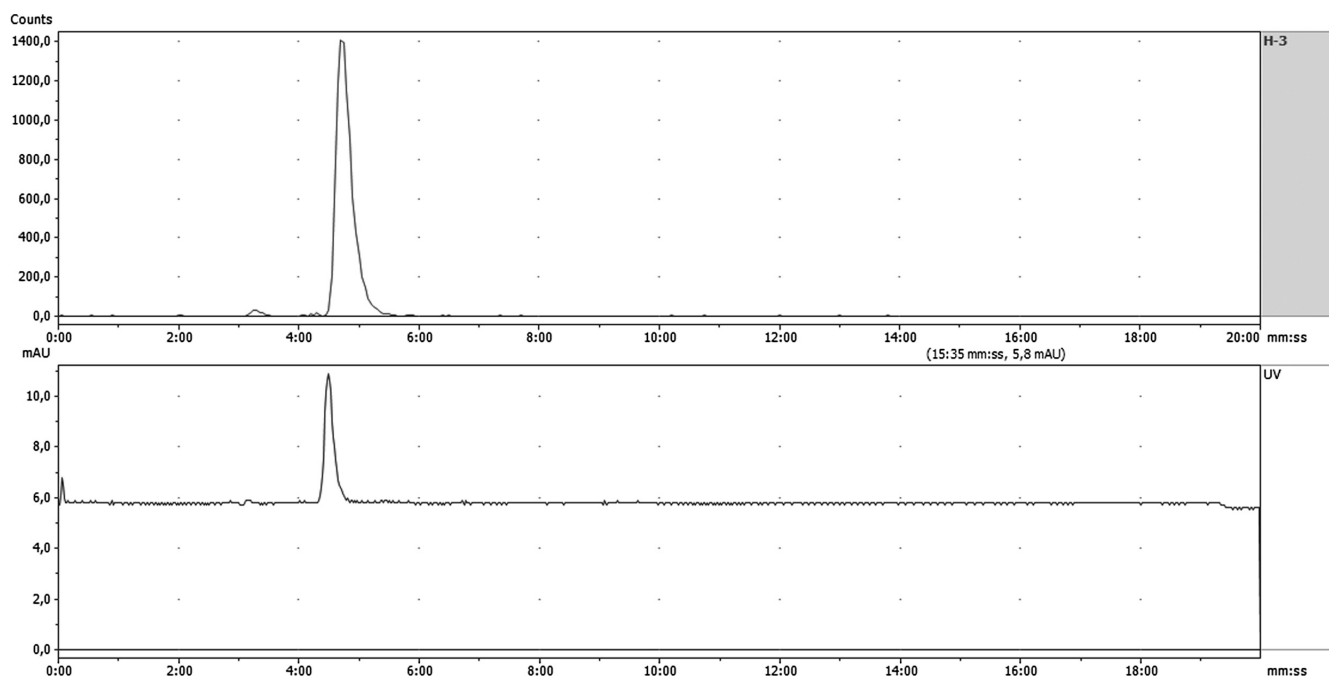


FIGURE 2 Analytical HPLC chromatogram of [³H]GMOM. The upper panel shows the radioactivity channel, the lower panel is the UV channel, spiked with unlabeled GMOM. Radiochemical and chemical purity was $>99\%$

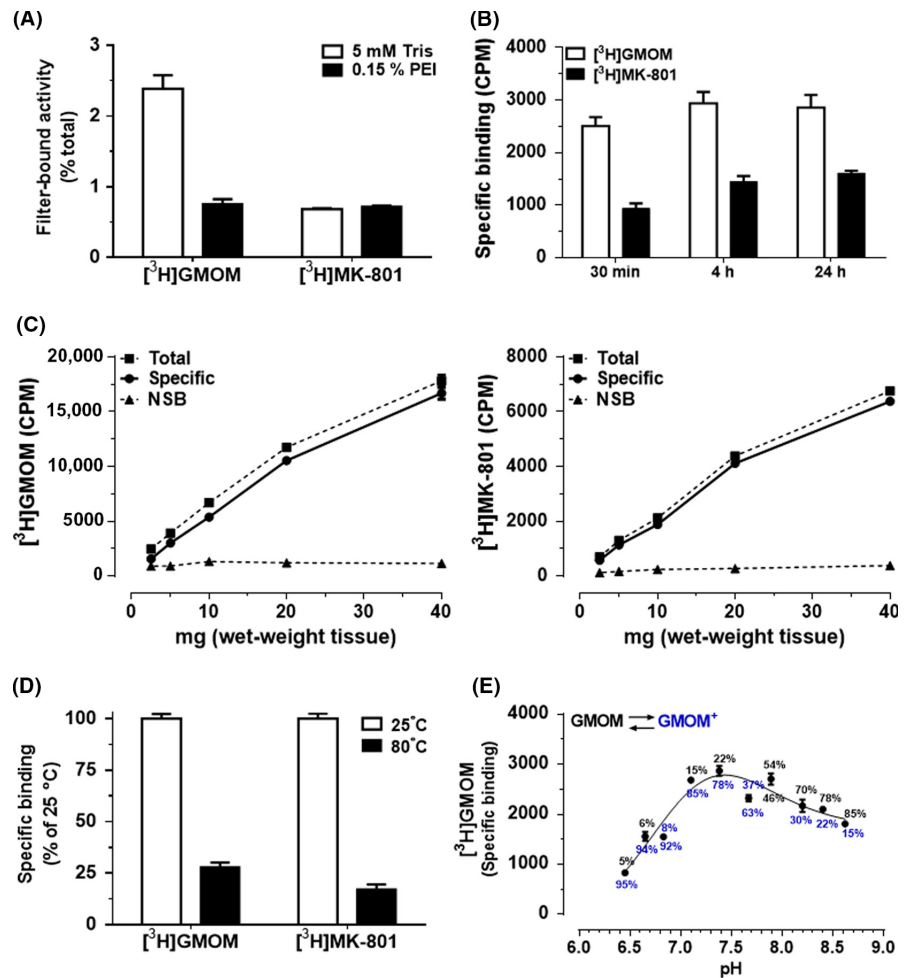


FIGURE 3 Evaluation of optimal binding conditions. A, Pretreatment of GF/B filters in 0.15% PEI for 1 hours reduces non-specific $[^3\text{H}]$ GMOM binding. B, The binding of $[^3\text{H}]$ GMOM and $[^3\text{H}]$ MK-801 is stable for at least 24 hours at 25°C. C, Tissue dilution curves were constructed to avoid radioligand depletion in subsequent studies. D, The binding of $[^3\text{H}]$ GMOM and $[^3\text{H}]$ MK-801 is heat-labile. E, For $[^3\text{H}]$ GMOM, maximum, pH-corrected specific binding occurs at pH 7.4. Percentages in black and blue correspond to the proportion of non-protonated and protonated species of GMOM at different pH values, respectively

3.5 | Homologous inhibition assays

Saturation binding parameters were obtained by self-inhibition of $[^3\text{H}]$ GMOM and $[^3\text{H}]$ MK-801 by increasing concentrations of unlabeled GMOM and MK-801, respectively. The assays were conducted in the absence and presence of L-glutamate ($100 \mu\text{mol L}^{-1}$), glycine ($30 \mu\text{mol L}^{-1}$), and combined L-glutamate/glycine. Table 2 shows B_{max} and K_d values of $[^3\text{H}]$ GMOM and $[^3\text{H}]$ MK-801, estimated by non-linear regression analysis with a one-site homologous competition model.

$[^3\text{H}]$ GMOM labeled more binding sites under baseline conditions compared to $[^3\text{H}]$ MK-801 ($P < 0.05$, LSD post-hoc tests). In the presence of combined L-glutamate and glycine, the B_{max} of $[^3\text{H}]$ GMOM ($P = 0.01$) and $[^3\text{H}]$ MK-801 ($P < 0.01$) increased over baseline, and was not different between radioligands ($P > 0.05$). Similarly, B_{max} values were not different between $[^3\text{H}]$ GMOM and $[^3\text{H}]$ MK-801 in the presence of L-glutamate or glycine alone ($P > 0.05$). Agonist-induced effects on baseline binding density were more pronounced for $[^3\text{H}]$ MK-801 than $[^3\text{H}]$ GMOM. L-glutamate ($P < 0.01$) and glycine ($P < 0.05$) enhanced the maximal binding of $[^3\text{H}]$ MK-801 by 131% and 92% over baseline, respectively. Under paired experimental conditions, the binding of $[^3\text{H}]$ GMOM was increased by less than 40% over baseline ($P > 0.05$). Two-way ANOVA confirmed significant main effects of

radioligand type ($F_{1,25} = 5.5$; $P < 0.05$) and agonist ($F_{3,25} = 8.2$; $P < 0.001$) on the B_{max} values of $[^3\text{H}]$ GMOM and $[^3\text{H}]$ MK-801.

Two-way ANOVA showed significant main effects of radioligand type ($F_{1,25} = 14.2$; $P < 0.001$) and agonist ($F_{3,25} = 5.3$; $P < 0.01$) on the apparent dissociation constants of $[^3\text{H}]$ GMOM and $[^3\text{H}]$ MK-801. The K_d value of $[^3\text{H}]$ GMOM was higher than that of $[^3\text{H}]$ MK-801 under baseline conditions (14.3 nmol L^{-1} vs 6.3 nmol L^{-1} ; $P < 0.01$, LSD post-hoc tests), and was decreased over baseline in the presence of L-glutamate ($P < 0.01$), glycine ($P < 0.01$) and combined L-glutamate/glycine ($P < 0.05$). For $[^3\text{H}]$ MK-801, the agonists induced a 4-fold decrease in mean K_d values compared to baseline, which did not reach statistical significance by two-way ANOVA ($P = 0.14$; LSD post-hoc tests). By one-way ANOVA, the effects of L-glutamate, glycine, and combined L-glutamate/glycine on the dissociation constants of $[^3\text{H}]$ MK-801 were significant (agonist effect: $F_{3,11} = 7.8$; $P < 0.01$; LSD post-hoc tests: $P < 0.01$ vs baseline).

Representative inhibition curves under baseline and combined agonist conditions are shown in Figure 5. Although the GMOM/ $[^3\text{H}]$ GMOM and MK-801/ $[^3\text{H}]$ MK-801 inhibition curves were fit significantly better by one-site rather than two-site competition models, Scatchard transformation of specific radioligand binding produced concave-upward curves for both $[^3\text{H}]$ GMOM and $[^3\text{H}]$ MK-801, under

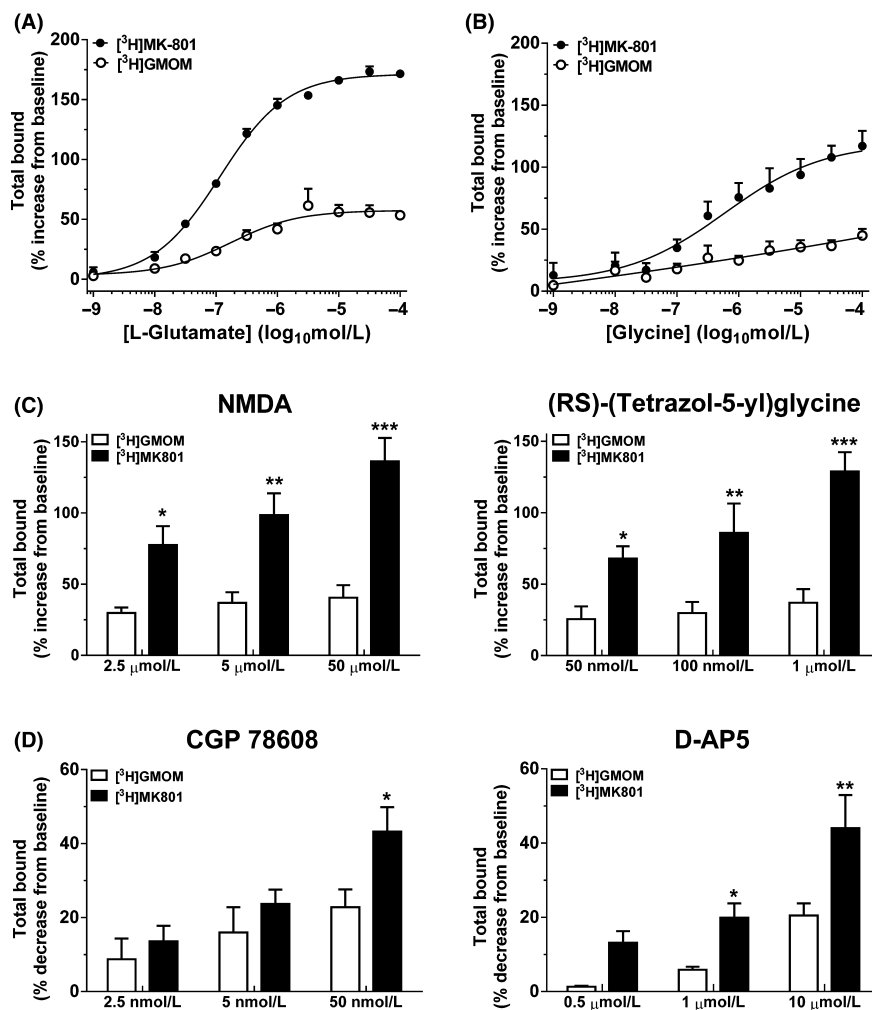


FIGURE 4 Regulation of radioligand binding by orthosteric NMDA receptor agonists/antagonists. Repeatedly washed, crude synaptic membranes were prepared from rat brain and immediately incubated with [³H]GMOM and [³H]MK-801 for ~20 hours, in the presence and absence of NMDA receptor agonists/antagonists. A, Maximal L-glutamate-induced increases over baseline were 3-fold lower for the binding of [³H]GMOM compared to [³H]MK-801. B, [³H]GMOM binding was increased in a linear, rather than exponential manner by increasing concentrations of glycine. C, NMDA and (RS)-(Tetrazol-5-yl)glycine were used at concentrations spanning ~1, 2 and 10× their respective affinity values for the GluN2 subunit of NMDA receptors, to confirm the differential sensitivity of [³H]GMOM and [³H]MK-801 to NMDA receptor agonism. D, The GluN1 subunit antagonist CGP 78608 and the GluN2 subunit antagonist D-AP5 decreased the binding of [³H]GMOM, albeit less than [³H]MK-801. Results are the mean ± SEM of 3-4 experiments, each conducted in triplicate. **P* < 0.05; ***P* < 0.01; ****P* < 0.001 vs [³H]GMOM, LSD post-hoc tests

TABLE 2 Saturation binding parameters of [³H]GMOM and [³H]MK-801, obtained by non-linear curve fitting

Condition	[³ H]GMOM			[³ H]MK-801		
	<i>K_d</i> (nmol L ⁻¹)	<i>B_{max}</i> (pmol/mg)	% increase from <i>B_{max}</i> baseline	<i>K_d</i> (nmol L ⁻¹)	<i>B_{max}</i> (pmol/mg)	% increase from <i>B_{max}</i> baseline
Baseline	14.3 ± 3.7 [†]	2.3 ± 0.4 [†]	0	6.3 ± 1.2	1.3 ± 0.3	0
+30 μmol L ⁻¹ Glycine	6.4 ± 0.4**	3.0 ± 0.2	30.4	1.6 ± 0.3	2.5 ± 0.2*	92.3
+100 μmol L ⁻¹ L-glutamate	5.4 ± 0.8**	3.1 ± 0.1	34.8	1.4 ± 0.1	3.0 ± 0.1**	130.8
+100 μmol L ⁻¹ L-glutamate/ 30 μmol L ⁻¹ Glycine	7.6 ± 0.9*	3.4 ± 0.2**	47.8	1.4 ± 0.2	2.9 ± 0.1**	123.1

Apparent affinity values (*K_d*) and maximum number of binding sites (*B_{max}*) were obtained by homologous inhibition assays, which were conducted in parallel for [³H]GMOM and [³H]MK-801 under each incubation condition. The results represent the mean ± SEM of 4-6 independent experiments, each conducted in triplicate. Following 20 hours incubations in extensively washed rat brain membranes, [³H]GMOM recognized more binding sites compared to [³H]MK-801 under baseline, but not combined L-glutamate/glycine conditions. [†]*P* < 0.05 vs baseline [³H]MK-801; **P* < 0.05; ***P* < 0.01 vs respective baseline conditions (two-way ANOVA, followed by LSD post-hoc tests).

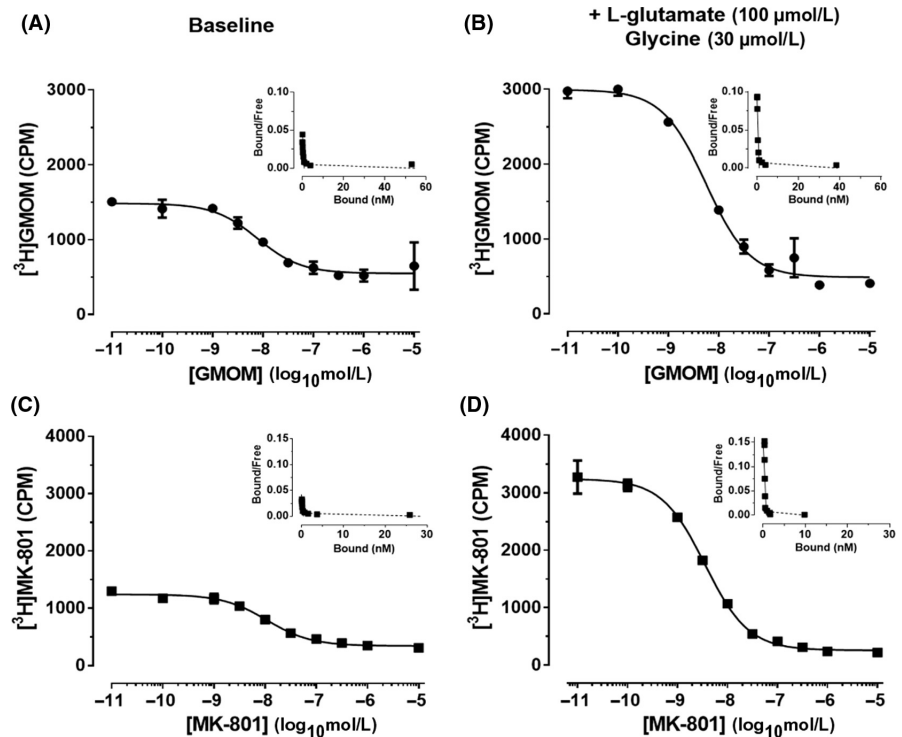
all incubation conditions examined (Figure 5 inserts). The region of the Scatchard plot with steep slope, representing high-affinity radioligand binding, accounted for ~2% of the binding sites labeled by [³H]GMOM and [³H]MK-801.

Linear regression of Scatchard-transformed data was performed to evaluate the *K_d* and *B_{max}* values of the two binding components (Table S2). Agonist-induced effects were observed on the high-affinity binding parameters of [³H]GMOM and [³H]MK-801.

3.6 | Heterologous inhibition assays

Inhibition curves of MK-801, memantine, (R,S)-ketamine and CNS-5161 against 3 nmol L⁻¹ and 10 nmol L⁻¹ [³H]GMOM were constructed in both absence and presence of 100 μmol L⁻¹ L-glutamate and 30 μmol L⁻¹ glycine. Under paired experimental conditions, GMOM, memantine, ketamine, and CNS-5161 were tested against 2 nmol L⁻¹ [³H]MK-801. The results are summarized in Table 3.

FIGURE 5 Homologous inhibition curves. Inhibition of the binding of [³H]GMOM (A and B, SA: 84.5 Ci/mmol) and [³H]MK-801 (C and D; SA: 22.5 Ci/mmol) by increasing concentrations of unlabeled GMOM and MK-801, respectively, under baseline (A and C) and combined agonist conditions (B and D). The inserts show Scatchard plots of [³H]GMOM and [³H]MK-801, obtained by transformation of homologous binding data by using 100 μmol L⁻¹ of unlabeled ligand to define NSB. Repeatedly washed preparations from the rat cortex and hippocampus were incubated with the radioligands for a period of 20 hours. Mean radioactivity counts added were 32 196 ± 1316 for 1 nmol L⁻¹ [³H]GMOM and 21 610 ± 1516 for 2 nmol L⁻¹ [³H]MK-801. Radioligand depletion was <10% for [³H]GMOM. For [³H]MK-801, under combined agonist conditions, maximum observed radioligand depletion was 16%



MK-801, memantine, and ketamine inhibited the binding of 3 nmol L⁻¹ [³H]GMOM with dual affinity under baseline conditions (Figure 6). The percentage of the low-affinity inhibition component was ~30% for MK-801 and ketamine, and 19% for memantine. The potency of memantine ($t_5 = 2.3$; $P = 0.07$) and ketamine ($t_5 = 2.4$; $P = 0.06$) for the high-affinity binding component of [³H]GMOM tended to decrease in the presence of L-glutamate/glycine compared to baseline, while that of MK-801 tended to increase ($t_7 = 1.9$; $P = 0.10$). There were no significant agonist-induced effects on the low-affinity IC₅₀ values of ketamine ($t_5 = 0.7$; $P > 0.05$), memantine ($t_5 = 0.4$; $P > 0.05$) and MK-801 ($t_7 = 1.3$; $P > 0.05$). CNS-5161 inhibited 3 nmol L⁻¹ [³H]GMOM in a monophasic manner under baseline conditions. A biphasic inhibition of [³H]GMOM by CNS-5161 was observed in the presence of L-glutamate/glycine.

The fraction of sites with high affinity for MK-801 ($t_8 = 3.6$; $P < 0.01$), ketamine ($t_5 = 6.0$; $P < 0.01$), memantine ($t_6 = 2.6$; $P < 0.05$), and CNS-5161 ($t_7 = 5.1$; $P < 0.01$) decreased when the inhibition assays were performed with 10 nmol L⁻¹ instead of 3 nmol L⁻¹ [³H]GMOM. The produced inhibition curves were shallower. The potency of MK-801 and memantine vs the high- and low-affinity binding components of [³H]GMOM decreased by a factor of two at 10 nmol L⁻¹ vs 3 nmol L⁻¹ of radioligand (MK-801: IC_{50-HIGH} $t_8 = 1.9$; $P = 0.09$, IC_{50-LOW} $t_8 = 1.0$; $P > 0.05$; memantine: IC_{50-HIGH} $t_6 = 2.1$; $P = 0.09$, IC_{50-LOW} $t_6 = 2.0$; $P = 0.10$). The opposite trend was observed for ketamine (IC_{50-HIGH} $t_5 = 1.6$; $P > 0.05$, IC_{50-LOW} $t_5 = 0.7$; $P > 0.05$, Table 3). CNS-5161 was less potent against the high ($t_7 = 2.4$; $P < 0.05$) and low ($t_7 = 2.8$; $P < 0.05$) affinity binding components of [³H]GMOM at 10 nmol L⁻¹ vs 3 nmol L⁻¹.

Under both baseline and L-glutamate/glycine conditions, the rank order of relative potency for the inhibition of [³H]MK-801 was CNS-

5161 > GMOM >> memantine > ketamine. In the presence of L-glutamate and glycine, memantine ($t_8 = 4.0$; $P < 0.01$) and ketamine ($t_{10} = 2.9$; $P < 0.05$) were less potent in competing for the [³H]MK-801 binding site compared to baseline conditions, by a factor of 3.4. The IC₅₀ values of GMOM ($t_{15} = 0.6$; $P > 0.05$) and CNS-5161 ($t_8 = 0.9$; $P > 0.05$) against [³H]MK-801 were not different in the presence and absence of agonist. Hill slopes (nH) close to unity were observed in all cases.

3.7 | Association kinetics

Association curves were constructed in the presence of 100 μmol L⁻¹ L-glutamate and 30 μmol L⁻¹ glycine, by using 5 nmol L⁻¹, 10 nmol L⁻¹, and 20 nmol L⁻¹ of [³H]GMOM, and 1 nmol L⁻¹, 2.5 nmol L⁻¹, and 5 nmol L⁻¹ of [³H]MK-801. Observed association rate constants (k_{ob}) for each radioligand concentration were derived by analyzing total, as well as specific binding values, which were determined in the presence of 500 μmol L⁻¹ (R,S)-ketamine (Table 4).

Analysis of total binding data revealed biphasic kinetics of association for [³H]GMOM and [³H]MK-801 at all examined concentrations (Figure 7A). The slow and fast rate constants did not follow a simple mass-action model, as k_{ob} values did not increase linearly with increasing radioligand concentration. Nevertheless, there was interdependency between the concentration-induced changes in the fast and slow association components of [³H]GMOM and [³H]MK-801 (Figure 7B). Thus, increased slow k_{ob} values were associated with decreased rates of fast association at increasing radioligand concentrations, and *vice versa* at 20 nmol L⁻¹ [³H]GMOM. The fraction of binding that was accounted for by the fast component of association

TABLE 3 Heterologous inhibition of [³H]GMOM and [³H]MK-801 by NMDA receptor ion-channel blockers

Condition	[³ H]GMOM (3 nmol L ^{-1,a} /10 nmol L ^{-1,b})				[³ H]MK-801 (2 nmol L ⁻¹)	
	vs MK-801				vs GMOM	
	IC ₅₀ High (nmol L ⁻¹)	IC ₅₀ Low (μmol L ⁻¹)	nH	% binding with high affinity	IC ₅₀ (nmol L ⁻¹)	nH
Baseline	4.1 ± 0.7 ^a	2.1 ± 1.0 ^a	-0.5 ± 0.1 ^a	70.1 ± 3.8 ^a	18.2 ± 3.1	1.1 ± 0.1
L-Glut/Glyc	2.5 ± 0.5 ^a	4.3 ± 1.3 ^a	-0.6 ± 0.1 ^a	77.4 ± 3.2 ^a	20.6 ± 2.0	1.0 ± 0.1
	5.1 ± 1.3 ^b	7.7 ± 3.2 ^b	-0.3 ± 0.1 ^b	58.9 ± 4.1 ^{b,**}		
	vs Memantine				vs Memantine	
	IC ₅₀ High (nmol L ⁻¹)	IC ₅₀ Low (μmol L ⁻¹)	nH	% binding with high affinity	IC ₅₀ (nmol L ⁻¹)	nH
Baseline	393 ± 18 ^a	298 ± 97 ^a	-0.7 ± 0.1 ^a	80.9 ± 5.9 ^a	393 ± 71	1.1 ± 0.0
L-Glut/Glyc	509 ± 41 ^a	377 ± 134 ^a	-0.7 ± 0.0 ^a	77.7 ± 3.5 ^a	1331 ± 145 ^{††}	0.9 ± 0.1
	1053 ± 261 ^b	643 ± 23 ^b	-0.4 ± 0.1 ^{b,***}	65.0 ± 3.5 ^{b,*}		
	vs Ketamine				vs Ketamine	
	IC ₅₀ High (nmol L ⁻¹)	IC ₅₀ Low (mmol L ⁻¹)	nH	% binding with high affinity	IC ₅₀ (nmol L ⁻¹)	nH
Baseline	563 ± 65 ^a	2.6 ± 1.2 ^a	-0.7 ± 0.0 ^a	70.4 ± 11.0 ^a	526 ± 98	0.7 ± 0.1
L-Glut/Glyc	937 ± 162 ^a	1.5 ± 0.8 ^a	-0.8 ± 0.1 ^a	88.7 ± 2.3 ^{a,*}	1771 ± 290 [†]	1.1 ± 0.1
	529 ± 180 ^b	0.9 ± 0.5 ^b	-0.5 ± 0.0 ^{b,*}	67.1 ± 2.6 ^{b,**}		
	vs CNS-5161				vs CNS-5161	
	IC ₅₀ High (nmol L ⁻¹)	IC ₅₀ Low (μmol L ⁻¹)	nH	% binding with high affinity	IC ₅₀ (nmol L ⁻¹)	nH
Baseline	4.4 ± 0.5 ^a	Not detected ^a	-0.9 ± 0.0 ^a	100 ^a	3.2 ± 0.4	1.0 ± 0.1
L-Glut/Glyc	2.2 ± 0.4 ^a	1.8 ± 1.1 ^a	-0.7 ± 0.0 ^a	84.2 ± 1.7 ^a	4.1 ± 0.8	1.0 ± 0.1
	10.6 ± 3.9 ^{b,*}	13.2 ± 4.5 ^{b,*}	-0.5 ± 0.1 ^{b,*}	68.3 ± 2.8 ^{b,**}		

[³H]GMOM (3 nmol L^{-1,a} and 10 nmol L^{-1,b}) and [³H]MK-801 (2 nmol L⁻¹) were incubated with increasing concentrations of ion-channel ligands in repeatedly washed rat brain membranes for a period of 20 hours, under baseline conditions and in the presence of 100 μmol L⁻¹ L-glutamate/30 μmol L⁻¹ glycine. Inhibition curves were analyzed after consideration of one- and two-site inhibition models in GraphPad Prism. [³H]GMOM was inhibited in a biphasic manner by MK-801, memantine and (*R,S*)-ketamine in both absence and presence of NMDA receptor agonists. Under paired experimental conditions, [³H]MK-801 was inhibited in a monophasic manner by GMOM, memantine, (*R,S*)-ketamine and CNS-5161. Results represent the mean ± SEM of 3–9 independent experiments, each conducted in triplicate. [†]*P* < 0.05, ^{††}*P* < 0.01 vs baseline condition; **P* < 0.05, ***P* < 0.01, ****P* < 0.001 vs 3 nmol L⁻¹ [³H]GMOM (independent two-tailed tests).

increased from 54.3 ± 2.3% at 5 nmol L⁻¹, to 58.6 ± 3.7% at 10 nmol L⁻¹, and 64.5 ± 2.4% at 20 nmol L⁻¹ of [³H]GMOM (concentration × Ymax interaction: *F*_{2,6} = 12.5; *P* < 0.01; repeated measures ANOVA). For 1 nmol L⁻¹ and 5 nmol L⁻¹ [³H]MK-801, 30.3 ± 5.0% and 38.2 ± 3.0% of total radioligand binding occurred in the fast phase, respectively (concentration × Ymax interaction: *F*_{2,6} = 2.0; *P* > 0.05).

Analysis of specific binding values, derived by subtracting the binding remaining in the presence of 500 μmol L⁻¹ (*R,S*)-ketamine from total binding values, revealed bi-exponential association kinetics for [³H]GMOM and [³H]MK-801 (Figure 7C and D). The observed rate constant values of specific binding were overall lower than those derived by analyzing total binding values, for both [³H]GMOM (*F*_{1,12} = 21.1; *P* < 0.001) and [³H]MK-801 (*F*_{1,12} = 6.3; *P* < 0.05). For both [³H]GMOM (*F*_{1,12} = 21.0; *P* < 0.001) and [³H]MK-801 (*F*_{1,12} = 6.1; *P* < 0.05), the reduction was due to decreases in the fast, rather than the slow phase of radioligand association. Decreased fast rate constants by total vs specific binding analysis were observed at 5 and 20 nmol L⁻¹ [³H]GMOM, and 1 nmol L⁻¹ [³H]MK-801 (LSD post-hoc tests).

4 | DISCUSSION

4.1 | Reduced open-channel dependence of [³H]GMOM

In extensively washed rat brain preparations, L-glutamate and glycine elevate the binding of [³H]MK-801²⁷ and [³H]TCP²⁸ with EC₅₀ values in the low μmol L⁻¹ range, that is consistent with the values herein reported for the stimulation of [³H]MK-801 binding. Agonist-induced increases in the binding of [³H]MK-801 have been proposed to reflect increased ligand affinity for the activated NMDA receptor state.^{5,6,27} In the present study, glutamate-induced increases in the baseline binding levels of [³H]GMOM (10 nmol L⁻¹) were three times lower compared to [³H]MK-801 (2.5 nmol L⁻¹). Increased radioligand binding was associated with a 2-fold increase in the baseline affinity of [³H]GMOM, which is lower than the 4-fold increase in the baseline affinity of [³H]MK-801. Thus, affinity-based mechanisms, likely associated with agonist-induced opening of the NMDA receptor channel, may contribute to the reduced open channel dependence of [³H]GMOM vs [³H]MK-801.

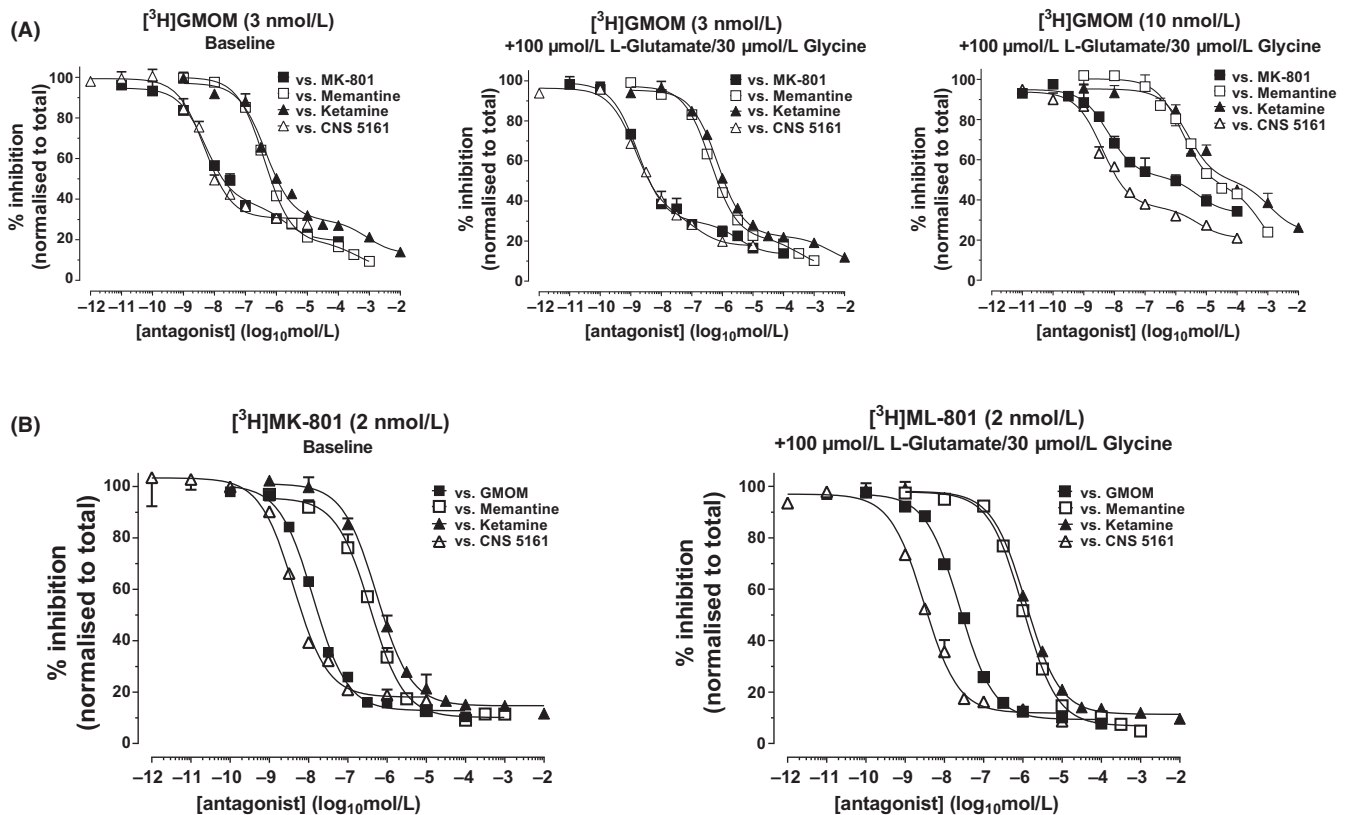


FIGURE 6 Inhibition curves of [³H]GMOM and [³H]MK-801 by NMDA receptor ion-channel blockers. Best-fit curves to one- or two-site models for the inhibition of [³H]GMOM (A) and [³H]MK-801 (B) are shown for baseline and agonist-stimulated conditions. Model preference was confirmed by visual inspection of the inhibition curves, and by the Akaike method. Each point is the mean \pm SEM of triplicate determinations from single experiments, repeated 3-9 independent times. Mean total bound [³H]GMOM (3 nmol L⁻¹) and [³H]MK-801 (2 nmol L⁻¹) under baseline conditions was 2216 ± 442 and 1137 ± 135 fmol per mg protein, respectively. In the presence of agonists, mean total bound [³H]GMOM (3 nmol L⁻¹) and [³H]MK-801 (2 nmol L⁻¹) were 2733 ± 208 and 2615 ± 124 fmol per mg protein, respectively

The decreased sensitivity of [³H]GMOM to NMDA receptor agonism may be further attributed to higher levels of binding at baseline, relative to agonist-stimulated conditions. Although the B_{max} of [³H]GMOM vs [³H]MK-801 was not different in the presence of L-glutamate and/or glycine, [³H]GMOM attained ~70% of its maximal, agonist-mediated binding at baseline, recognizing more binding sites than [³H]MK-801 exclusively in the absence of added agonists. Assuming that equilibrium conditions were approached following 20 hours incubation times,^{22,29} these findings indicate ease of [³H]GMOM binding to non-stimulated, closed NMDA receptor conformations, relative to [³H]MK-801. Perhaps the recognition site for the binding of [³H]GMOM to NMDA receptors is shallower than that of [³H]MK-801, similar to what has been reported for [³H]dextrorphan.³⁰ The differential regulation of the binding of [³H]GMOM and [³H]MK-801 by orthosteric agonists/antagonists would be consistent with this suggestion.

4.2 | Non-linear Scatchard plots

Linear transformation of homologous inhibition data produced concave upward curves for [³H]GMOM and [³H]MK-801, indicating binding to a heterogeneous population of sites, negative co-

operativity, or a significant non-specific component.³¹ Multiple components of [³H]MK-801 binding have been reported previously, in studies using extensively washed synaptosomal preparations from the rat³² and human brain.³³⁻³⁵ Moreover, electrophysiological studies of primary hippocampal neurons have shown that MK-801 blocks NMDA-induced currents with both high- and low-affinity, in a voltage-dependent manner.³⁶ Although there is variation in [³H]MK-801's low-affinity K_d value between studies, which extends from the low nmol L⁻¹ to the μ mol L⁻¹ range, the present results and the aforementioned literature support a complex model for the binding of [³H]GMOM and [³H]MK-801.

A low-affinity binding component for [³H]MK-801 has not been reported consistently in the literature.^{5,37,38} The present study shows that this discrepancy extends to the diarylguanidine class of radioligands. Unlike [³H]GMOM, [³H]CNS-5161 has been shown to yield a single affinity element after 90 minutes incubations with native NMDA receptors, at a concentration range between 0.1 and 2.5 nmol L⁻¹.³⁹ These data imply that radioligand concentration and the duration of incubation may be important variables in detecting the multiple affinity components of [³H]MK-801 and [³H]GMOM in saturation experiments.

TABLE 4 Observed association rate constants (k_{ob}) of [3 H]GMOM and [3 H]MK-801

Component	[3 H]GMOM				[3 H]MK-801							
	5 nmol L $^{-1}$		10 nmol L $^{-1}$		20 nmol L $^{-1}$		1 nmol L $^{-1}$		2.5 nmol L $^{-1}$		5 nmol L $^{-1}$	
	Total	Specific	Total	Specific	Total	Specific	Total	Specific	Total	Specific	Total	Specific
Fast (min $^{-1}$)	2.9 ± 1.1	0.7 ± 0.1*	2.6 ± 0.5	1.4 ± 0.1	4.4 ± 0.9	1.0 ± 0.3*	2.5 ± 0.7	1.0 ± 0.2*	2.2 ± 0.8	1.1 ± 0.5	2.0 ± 0.3	1.3 ± 0.4
Slow (min $^{-1}$ × 10 $^{-3}$)	22.2 ± 5.4	20.4 ± 5.8	28.8 ± 2.9	26.0 ± 3.1	17.4 ± 11.4	22.4 ± 8.0	21.8 ± 3.7	17.0 ± 1.4	23.7 ± 4.4	19.4 ± 3.2	27.2 ± 6.0	22.2 ± 3.2

Results represent the mean ± SEM of three independent association experiments, each performed using three concentrations of [3 H]GMOM and [3 H]MK-801 and conducted in triplicate. Observed rate constants were determined in the presence of 100 μ mol L $^{-1}$ L-glutamate and 30 μ mol L $^{-1}$ glycine. Time-points ranging from 30 seconds to 300 minutes were evaluated. Results were derived by analyzing total, as well as specific binding values, determined in the presence of 500 μ mol L $^{-1}$ (R,S)-ketamine. Both fast and slow components of association were observed for the binding of [3 H]GMOM and [3 H]MK-801. * p < 0.05 vs Total binding values, LSD post-hoc tests.

4.3 | Biphasic inhibition curves by ion-channel ligands

For [3 H]MK-801, the observed potency of inhibition by ketamine,^{40,41} memantine,^{40,42} GMOM,^{1,3} and CNS-5161⁴³ is within the range reported from previous binding studies, conducted in the presence of L-glutamate and glycine on rat brain membranes. For [3 H]GMOM, the open-channel blockers produced inhibition curves with slope factors smaller than unity and clear inflection points, observations that are not compatible with displacement from a homogeneous population of non-interacting sites. The complex curves are unlikely to reflect inhibition of [3 H]GMOM from populations other than the NMDA receptor, or from distinct subtypes of NMDA receptors, with different affinity. Observations to support this statement include GMOM's selectivity profile at 3 nmol L $^{-1}$ and 10 nmol L $^{-1}$, the limited ability of MK-801, ketamine and memantine to discriminate between NMDA receptor subtypes,⁴⁴ and the fact that L-glutamate and glycine altered the potency of the tested compounds against the high- and low-affinity inhibition components of [3 H]GMOM. If different subtypes of NMDA receptors were to account for the dual affinity of MK-801 or ketamine, for example, the antagonists' high-to-low IC₅₀ ratio would be expected to be similar under baseline and agonist-stimulated conditions or at 3 vs 10 nmol L $^{-1}$ [3 H]GMOM. Therefore, a more likely explanation for the biphasic inhibition of [3 H]GMOM is that multiple sites on one set of receptors, presumably the NMDA receptor ionophore, are involved in the binding of the ion-channel blockers.

Comparison of inhibitor IC₅₀ values in the absence and presence of exogenous L-glutamate/glycine revealed that the agonists rendered memantine and ketamine less potent in inhibiting [3 H]MK-801 compared to baseline, a tendency that was also observed against the high-affinity binding component of [3 H]GMOM. It is possible that [3 H]MK-801's slow kinetics vs memantine and ketamine may have overestimated the blockers' potency under baseline conditions, even following 20 hours incubation periods. However, the IC₅₀ of GMOM and CNS-5161 vs [3 H]MK-801 was not different in the absence and presence of agonists, which is indicative of equilibrium binding conditions. Thus, it is likely that a decrease in the affinity of ketamine and memantine for the agonist-bound NMDA receptor may contribute to their channel-blocking properties. Although memantine's IC₅₀ value vs [3 H]MK-801 is consistent with the drug's anticipated brain concentrations at therapeutically relevant doses,⁴⁵ the significance of these findings and whether they relate to therapeutic index in vivo is unknown.

It would appear, however, that [3 H]GMOM provides information on the interaction of ion-channel ligands with NMDA receptors that is not obtained with low concentrations of [3 H]MK-801. This is evidenced by the fact that, in the presence of L-glutamate/glycine, the potency of the tested drugs against [3 H]MK-801 is a combination of their high and low IC₅₀ values against [3 H]GMOM.

4.4 | Bi-exponential association kinetics

Biphasic association curves for the binding of [3 H]MK-801 have been described previously.^{22,38,46,47} The present data extend the

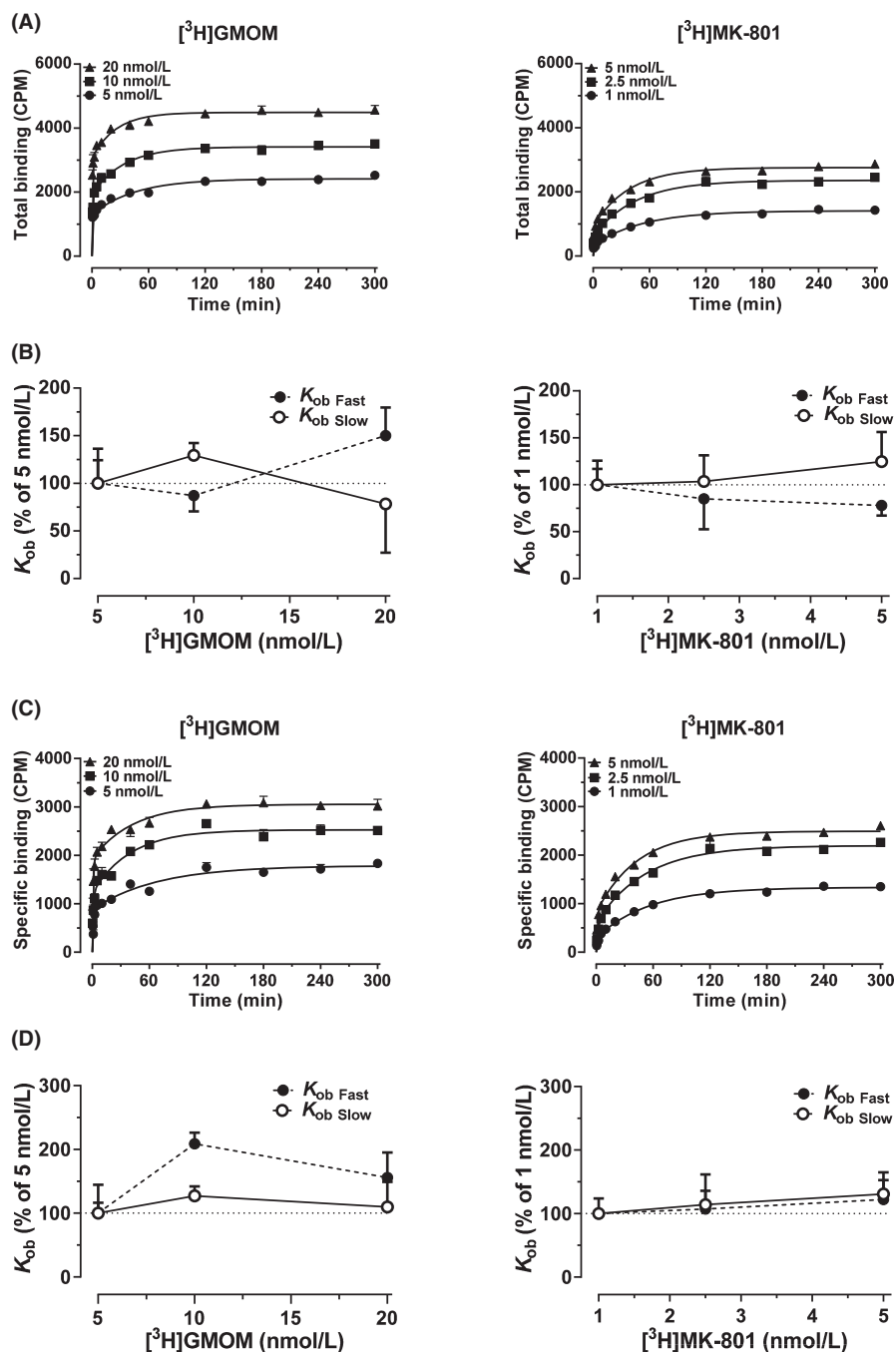


FIGURE 7 Association kinetics of [3 H]GMOM and [3 H]MK-801. Representative association curves and concentration-induced changes in the observed kinetic rate constants (k_{ob}) of [3 H]GMOM and [3 H]MK-801, derived by analysis of total (A and B) and specific (C and D) radioligand binding values. The fast and slow k_{ob} values of total radioligand binding changed in opposite directions by increasing the concentration of radioligand (B). Analysis of specific binding, determined in the presence of $500 \mu\text{mol L}^{-1}$ ketamine, revealed concentration-induced increases in the fast rather than slow association phase of radioligand binding (D)

detection of multiple association components to the diarylguanidine class of compounds. To date, only a handful of studies have examined how the observed rate constants of ion-channel blockers change as a function of radioligand concentration. For [3 H]MK-801, evidence suggests that the kinetics of binding in repeatedly washed rat brain preparations both follow²² and deviate³⁷ from the simple law of mass-action.

Under combined agonist conditions, it has been proposed that the fast association component of [3 H]MK-801 represents binding to the open NMDA channel, while the slow component represents a different route by which the radioligand associates with its binding site,

likely corresponding to closed or desensitized NMDA receptor conformations.^{22,38} The observation that the slow rate constants of [3 H]GMOM and [3 H]MK-801 were not different by analysis of total and specific binding values indicates that the slow association phase represents a non-specific process, perhaps associated with closed²² or desensitized NMDA receptor conformations.³⁸ However, the concept that fast and slow association rates represent binding to open and closed NMDA conformations, respectively, is not compatible with the concentration-induced changes favoring the fast phase of radioligand association, which were observed with 20 nmol L^{-1} [3 H]GMOM, or when analyzing data obtained with $500 \mu\text{mol L}^{-1}$ ketamine. A

functional, yet speculative interpretation of these results, considering multiple interacting sites on the NMDA receptor, is that the kinetics of ion-channel blockers are determined by occupancy of the sites exhibiting fast kinetics of radioligand binding (low-affinity sites for [³H]GMOM). In other words, the fast and slow components of association may be associated with both open and closed NMDA receptor conformations, depending on antagonist concentration.

4.5 | Relevance to [¹¹C]GMOM PET

In five out of six individuals that underwent dynamic PET scanning with [¹¹C]GMOM at baseline and following the administration of S-ketamine, the antagonist reduced [¹¹C]GMOM's net influx rate (K_i , slow component), indicating that the inward transport and/or trapping of the tracer was decreased compared to baseline.¹⁹ Interestingly, the decrease in K_i was coupled to increased values of non-displaceable distribution volume (V_{ND} , fast component) across the gray matter of the same five individuals, an increase that occurred in the absence of perfusion-dependent effects. Moreover, the administration of S-ketamine increased K_i over baseline in 1 out of 6 subjects. In that individual, V_{ND} was decreased. Thus, the V_{ND} parameter of [¹¹C]GMOM contains a component that is subject to regulation by S-ketamine, in a manner that is opposite to that of K_i . These results are reminiscent of the ketamine-induced alterations in the fast association rate of [³H]GMOM, and the interdependence between the fast and slow association rates of total [³H]GMOM binding.

5 | CONCLUSIONS

We report on the synthesis and in vitro binding properties of [³H]GMOM. Similar to MK-801⁴⁸ and the diarylguanidine tracers,^{15,39,43,49} GMOM is selective for the NMDA receptor ionophore. However, [³H]GMOM is inhibited by open-channel blockers in a biphasic manner, in both absence and presence of L-glutamate and glycine. The radioligand displays non-linear Scatchard curves and bi-exponential association kinetics, which are incompatible with the simple law of mass-action, involving binding to a homogeneous population of equivalent sites. These results indicate that NMDA-selective, nmol L⁻¹ concentrations of GMOM, such as those used in PET imaging studies, are unlikely to target a single intra-channel site that is primarily associated with the activated state of NMDA receptors.

ACKNOWLEDGEMENTS

This study received support from the Center for Translational Molecular Medicine (project LEARN, 02N-101), and the EU 7th framework program EURIPIDES (grant HEALTH-F5-2007-201380).

AUTHOR CONTRIBUTIONS

Participated in research design: A. M., B. N. M. v. B., A. D. W., J. E. L. Conducted experiments: A. M., J. V., E. C. N., E. J. M. K., V. A. R.,

J. E. L. Contributed new reagents or analytic tools: P. J. K., J. V., J. A. M. C. Performed data analysis: A. M., J. V., E. C. N., V. A. R., J. E. L. Wrote or contributed to writing of the manuscript: All authors.

ORCID

Athanasios Metaxas  <http://orcid.org/0000-0002-8747-7068>

REFERENCES

- Kassenbrock A, Vasdev N, Liang SH. Selected PET radioligands for ion channel linked neuroreceptor imaging: focus on GABA, NMDA and nACh receptors. *Curr Top Med Chem*. 2016;16(16):1830-1842.
- Sobrio F. Radiosynthesis of carbon-11 and fluorine-18 labelled radiotracers to image the ionotropic and metabotropic glutamate receptors. *J Labelled Comp Radiopharm*. 2013;56(3-4):180-186.
- Zhou Q, Sheng M. NMDA receptors in nervous system diseases. *Neuropharmacology*. 2013;74:69-75.
- Traynelis SF, Wollmuth LP, McBain CJ, et al. Glutamate receptor ion channels: structure, regulation, and function. *Pharmacol Rev*. 2010;62(3):405-496.
- Foster AC, Wong EH. The novel anticonvulsant MK-801 binds to the activated state of the N-methyl-D-aspartate receptor in rat brain. *Br J Pharmacol*. 1987;91(2):403-409.
- Reynolds IJ, Murphy SN, Miller RJ. 3H-labeled MK-801 binding to the excitatory amino acid receptor complex from rat brain is enhanced by glycine. *Proc Natl Acad Sci USA*. 1987;84(21):7744-7748.
- Waterhouse RN. Imaging the PCP site of the NMDA ion channel. *Nucl Med Biol*. 2003;30(8):869-878.
- Keana JF, McBurney RN, Scherz MW, et al. Synthesis and characterization of a series of diarylguanidines that are noncompetitive N-methyl-D-aspartate receptor antagonists with neuroprotective properties. *Proc Natl Acad Sci USA*. 1989;86(14):5631-5635.
- Fuchigami T, Nakayama M, Yoshida S. Development of PET and SPECT probes for glutamate receptors. *ScientificWorldJournal*. 2015;2015:716514.
- Orita K, Sasaki S, Maeda M, et al. Synthesis and evaluation of 1-(1-[5-(2'-[18F]fluoroethyl)-2-thienyl]-cyclohexyl)piperidine as a potential in vivo radioligand for the NMDA receptor-channel complex. *Nucl Med Biol*. 1993;20(7):865-873.
- Sihver S, Sihver W, Andersson Y, et al. In vitro and in vivo characterization of (+)-3-[11C]cyano-dizocilpine. *J Neural Transm (Vienna)*. 1998;105(2-3):117-131.
- Waterhouse RN, Dumont F, Sultana A, Simpson N, Laruelle M. Synthesis of [11C] N-(2-chloro-5-thiomethylphenyl)-N'-(3-methoxyphenyl)-N'-methylguanidine ([11C]GMOM): a candidate PET tracer for imaging the PCP site of the NMDA ion channel. *J Labelled Comp Radiopharm*. 2002;45(11):955-964.
- Klein PJ, Christiaans JA, Metaxas A, et al. Synthesis, structure activity relationship, radiolabeling and preclinical evaluation of high affinity ligands for the ion channel of the N-methyl-d-aspartate receptor as potential imaging probes for positron emission tomography. *Bioorg Med Chem*. 2015;23(5):1189-1206.
- Zhao Y, Robins E, Turton D, Brady F, Luthra SK, Årstad E. Synthesis and characterization of N-(2-chloro-5-methylthiophenyl)-N'-(3-methylthiophenyl)-N'-[11C]methylguanidine [11C]CNS 5161, a candidate PET tracer for functional imaging of NMDA receptors. *J Labelled Comp Radiopharm*. 2006;49(2):163-170.
- Robins EG, Zhao Y, Khan I, Wilson A, Luthra SK, Rstad E. Synthesis and in vitro evaluation of (18)F-labelled S-fluoroalkyl diarylguanidines: novel high-affinity NMDA receptor antagonists for imaging with PET. *Bioorg Med Chem Lett*. 2010;20(5):1749-1751.

16. Ahmed I, Bose SK, Pavese N, et al. Glutamate NMDA receptor dysregulation in Parkinson's disease with dyskinesias. *Brain*. 2011;134 (Pt 4):979-986.
17. McGinnity CJ, Hammers A, Riano Barros DA, et al. Initial evaluation of 18F-GE-179, a putative PET Tracer for activated N-methyl D-aspartate receptors. *J Nucl Med*. 2014;55(3):423-430.
18. van der Aart J, Golla SSV, van der Pluijm M, et al. First in human evaluation of [18F]PK-209, a PET ligand for the ion channel binding site of NMDA receptors. *EJNMMI Res*. 2018;8(1):69.
19. van der Doef TF, Golla SS, Klein PJ, et al. Quantification of the novel N-methyl-d-aspartate receptor ligand [11C]GMOM in man. *J Cereb Blood Flow Metab*. 2016;36(6):1111-1121.
20. Christiaans JA, Klein PJ, Metaxas A, et al. Synthesis and preclinical evaluation of carbon-11 labelled N-(5-(4-fluoro-2-[(11C)methoxyphenyl]pyridin-3-yl)methyl)cyclopentanamine as a PET tracer for NR2B subunit-containing NMDA receptors. *Nucl Med Biol*. 2014;41 (8):670-680.
21. Cheng Y, Prusoff WH. Relationship between the inhibition constant (K₁) and the concentration of inhibitor which causes 50 per cent inhibition (I₅₀) of an enzymatic reaction. *Biochem Pharmacol*. 1973;22(23):3099-3108.
22. Javitt DC, Zukin SR. Biexponential kinetics of [3H]MK-801 binding: evidence for access to closed and open N-methyl-D-aspartate receptor channels. *Mol Pharmacol*. 1989;35(4):387-393.
23. Ametamey SM, Kolic M, Carrey-Remy N, et al. Synthesis, radiolabelling and biological characterization of (D)-7-iodo-N-(1-phosphonoethyl)-5-aminomethylquinoxaline-2,3-dione, a glycine-binding site antagonist of NMDA receptors. *Bioorg Med Chem Lett*. 2000;10(1):75-78.
24. Kendrick SJ, Lynch DR, Pritchett DB. Characterization of glutamate binding sites in receptors assembled from transfected NMDA receptor subunits. *J Neurochem*. 1996;67(2):608-616.
25. Schoepp DD, Smith CL, Lodge D, et al. D, L-(tetrazol-5-yl) glycine: a novel and highly potent NMDA receptor agonist. *Eur J Pharmacol*. 1991;203(2):237-243.
26. Jeffries WB, Waugh D, Abel PW. Analysis of data from "cold saturation" radioligand binding experiments. *Methods Mol Biol*. 1997;73:331-342.
27. Ransom RW, Stec NL. Cooperative modulation of [3H]MK-801 binding to the N-methyl-D-aspartate receptor-ion channel complex by L-glutamate, glycine, and polyamines. *J Neurochem*. 1988;51(3):830-836.
28. Benavides J, Rivy JP, Carter C, Scatton B. Differential modulation of [3H]TCP binding to the NMDA receptor by L-glutamate and glycine. *Eur J Pharmacol*. 1988;149(1-2):67-72.
29. Reynolds IJ, Miller RJ. Multiple sites for the regulation of the N-methyl-D-aspartate receptor. *Mol Pharmacol*. 1988;33(6):581-584.
30. LePage KT, Ishmael JE, Low CM, Traynelis SF, Murray TF. Differential binding properties of [3H]dextrorphan and [3H]MK-801 in heterologously expressed NMDA receptors. *Neuropharmacology*. 2005;49(1):1-16.
31. Wilkinson KD. Quantitative analysis of protein-protein interactions. *Methods Mol Biol*. 2004;261:15-32.
32. Javitt DC, Zukin SR. Interaction of [3H]MK-801 with multiple states of the N-methyl-D-aspartate receptor complex of rat brain. *Proc Natl Acad Sci USA*. 1989;86(2):740-744.
33. Kornhuber J, Bormann J, Retz W, Hubers M, Riederer P. Memantine displaces [3H]MK-801 at therapeutic concentrations in postmortem human frontal cortex. *Eur J Pharmacol*. 1989a;166(3):589-590.
34. Kornhuber J, Mack-Burkhardt F, Kornhuber ME, Riederer P. [3H]MK-801 binding sites in post-mortem human frontal cortex. *Eur J Pharmacol*. 1989b;162(3):483-490.
35. Steele JE, Robinson TN, Cross AJ, Bowen DM, Green AR. A comparison of [3H]MK-801 and N-[1-(2-thienyl)cyclohexyl]-3,4-[3H]piperidine binding to the N-methyl-D-aspartate receptor complex in human brain. *J Neurochem*. 1991;56(4):1248-1254.
36. Vandame D, Desmadryl G, Becerril Ortega J, et al. Comparison of the pharmacological properties of GK11 and MK801, two NMDA receptor antagonists: towards an explanation for the lack of intrinsic neurotoxicity of GK11. *J Neurochem*. 2007;103(4):1682-1696.
37. Kloog Y, Nadler V, Sokolovsky M. Mode of binding of [3H]dibenzocloalkenimine (MK-801) to the N-methyl-D-aspartate (NMDA) receptor and its therapeutic implication. *FEBS Lett*. 1988;230(1-2):167-170.
38. Rajdev S, Reynolds IJ. Effects of pH on the actions of dizocilpine at the N-methyl-D-aspartate receptor complex. *Br J Pharmacol*. 1993;109(1):107-112.
39. Biegon A, Gibbs A, Alvarado M, Ono M, Taylor S. In vitro and in vivo characterization of [3H]CNS-5161—a use-dependent ligand for the N-methyl-D-aspartate receptor in rat brain. *Synapse*. 2007;61(8):577-586.
40. Bresink I, Danysz W, Parsons CG, Mutschler E. Different binding affinities of NMDA receptor channel blockers in various brain regions—indication of NMDA receptor heterogeneity. *Neuropharmacology*. 1995;34(5):533-540.
41. Wong EH, Knight AR, Woodruff GN. [3H]MK-801 labels a site on the N-methyl-D-aspartate receptor channel complex in rat brain membranes. *J Neurochem*. 1988;50(1):274-281.
42. Parsons CG, Quack G, Bresink I, et al. Comparison of the potency, kinetics and voltage-dependency of a series of uncompetitive NMDA receptor antagonists in vitro with anticonvulsant and motor impairment activity in vivo. *Neuropharmacology*. 1995;34(10):1239-1258.
43. Hu LY, Guo J, Magar SS, Fischer JB, Burke-Howie KJ, Durant GJ. Synthesis and pharmacological evaluation of N-(2,5-disubstituted phenyl)-N'-(3-substituted phenyl)-N'-methylguanidines as N-methyl-D-aspartate receptor ion-channel blockers. *J Med Chem*. 1997;40 (26):4281-4289.
44. Ogden KK, Traynelis SF. New advances in NMDA receptor pharmacology. *Trends Pharmacol Sci*. 2011;32(12):726-733.
45. Rammes G, Danysz W, Parsons CG. Pharmacodynamics of memantine: an update. *Curr Neuropharmacol*. 2008;6(1):55-78.
46. Reynolds IJ. 1,5-(Diethylamino)piperidine, a novel spermidine analogue that more specifically activates the N-methyl-D-aspartate receptor-associated polyamine site. *Mol Pharmacol*. 1992;41(6):989-992.
47. Williams K, Dawson VL, Romano C, Dichter MA, Molinoff PB. Characterization of polyamines having agonist, antagonist, and inverse agonist effects at the polyamine recognition site of the NMDA receptor. *Neuron*. 1990;5(2):199-208.
48. Wong EH, Kemp JA, Priestley T, Knight AR, Woodruff GN, Iversen LL. The anticonvulsant MK-801 is a potent N-methyl-D-aspartate antagonist. *Proc Natl Acad Sci USA*. 1986;83(18):7104-7108.
49. Golla SS, Klein PJ, Bakker J, et al. Preclinical evaluation of [(18F)PK-209, a new PET ligand for imaging the ion-channel site of NMDA receptors. *Nucl Med Biol*. 2015;42(2):205-212.

SUPPORTING INFORMATION

Additional supporting information may be found online in the Supporting Information section at the end of the article.

How to cite this article: Metaxas A, van Berckel BNM, Klein PJ, et al. Binding characterization of N-(2-chloro-5-thiomethylphenyl)-N'-(3-[³H]₃methoxy phenyl)-N'-methylguanidine ([³H]GMOM), a non-competitive N-methyl-D-aspartate (NMDA) receptor antagonist. *Pharmacol Res Perspect*. 2019;e00458. <https://doi.org/10.1002/prp.2.458>